

Rheological Aspects of Microbial Hyaluronic Acid

Aline M. B. Pires, Maria H. A. Santana

Laboratory of Development of Biotechnological Processes, School of Chemical Engineering, University of Campinas, UNICAMP, P.O. BOX 6066, 13083-852, Campinas, SP, Brazil

Received 7 September 2009; accepted 15 December 2010

DOI 10.1002/app.33976

Published online 19 April 2011 in Wiley Online Library (wileyonlinelibrary.com).

ABSTRACT: The rheological properties of the hyaluronic acid (HA) produced by the cultivation of *Streptococcus zooepidemicus* ATCC 39920 in synthetic medium at constant pH of 7.0 were determined. Relevant characteristics of the biopolymer as its pureness related to proteins (0.44 mg of protein per gram of HA) and its average molar weight (4.0×10^6 Da) were also determined. Experimental data in steady shear (flow curves) have been correlated with the Cross model, which described the apparent viscosity shear rate data well mainly at concentrations higher than 50 mg mL^{-1} . The concentration dependence of specific viscosity showed two linear regimes that intercept at critical overlap concentration

(c^*) equal to 4 mg mL^{-1} . The storage (G') and loss (G'') moduli increasing along the HA concentration and estimates out of the studied range indicate that a crossover frequency decreased with the increasing concentration of HA. The high concentration dependence of G' as well as the deviations of the Cox-Merz rule for most of the HA concentrations indicate the hyperentangled properties for the HA chains, which could be visualized through atomic force microscopy images even at low concentrations as 0.01 mg mL^{-1} . © 2011 Wiley Periodicals, Inc. *J Appl Polym Sci* 122: 126–133, 2011

Key words: rheology; viscoelastic properties; biopolymers

INTRODUCTION

The hyaluronic acid (HA) is a biocompatible and biodegradable polymer which was identified in connective tissues and certain prokaryotes. HA is a linear polysaccharide composed by repeating disaccharide units composed of *N*-acetylglucosamine and *D*-glucuronic acid linked by β -1-3 and β -1-4 glucosidic bonds. It has one carboxylate group per disaccharide unit, and is therefore a polyelectrolyte. HA is polydisperse with molecular weight ranging from 10^4 to 10^7 Da.¹

It is remarkable that HA shows high specificity and versatility interacting with proteoglycans, cell membranes, and receptors on a molecule-to-molecule basis.² Its biological functions include the maintenance of elastoviscosity of liquid connective tissues, control of tissue hydration and water transport, supramolecular assembly of proteoglycans in the extracellular matrix, and numerous receptor-mediated roles in cell detachment, mitosis, tumor development and metastasis, and inflammation.³

Despite the simple, well-defined chemical structure of HA and research on its properties solutions for over 60 years, the HA conformation in solution is still controversial.⁴ It may adopt different conformations depending on the level of hydration, the

ionic environment and the temperature.⁵ Thus, on the basis of hydrodynamic, spectroscopic and theoretical investigations, in dilute solution under physiological solvent conditions, HA chains adopt semiflexible random coil configurations.⁶ The chains occupy large hydrodynamic domains with a low density of chain segments, as a result of the high HA molecular weight, the local stiffness arising from the intrinsically large size of the monomeric units (sugar rings), the hindered rotations about the glycosidic linkages and the dynamically formed and broken interresidue hydrogen bonds.^{7,8}

Balazs and Gibbs⁹ showed that, at low frequencies, HA macromolecules have enough time to readjust themselves to the original conformation through the disentanglements of chain segments. Under this condition, the material response is essentially viscous. On the other hand, when HA is subjected to rapid deformation, at high frequencies, the entangled network structure can readjust itself very quickly and reform other entanglements giving rise to the overall elastic response of the material. These structural features account for the viscoelastic rheology and ability of the polymer to retain large volumes of water which are important in determining the HA functions.¹⁰

The biological specificities and remarkable viscoelastic properties make the HA an attractive biomaterial for various applications in ophthalmology,¹¹ rheumatology,¹² dermatology,¹³ pharmacology and drug delivery.¹⁴ In some applications, HA is cross-linked to alter its physical properties and resorption rate.¹⁵

Correspondence to: A. M. B. Pires (alinembpires@yahoo.com.br).

Contract grant sponsors: CNPq, FAPESP.

The rheological analysis is a useful tool to explore relationships between mechanical behavior and structure, concentration, and molecular weight of biopolymers solutions.¹⁶ Therefore, rheological properties provides valuable indications to better design proper substitutes for specific medical and cosmetic application. The rheological behaviors are of decisive importance for all applications.¹⁷

The aim of this work was to determine the main rheological properties of microbial HA produced by *Streptococcus zooepidemicus* ATCC 39920 cultivated at controlled pH 7.0 and precipitated with ethanol at the same pH. The conformation of polymer from solution was also observed by atomic force microscopy (AFM).

MATERIAL AND METHODS

HA production

The HA used in this study was produced by *Streptococcus equi* subsp. *zooepidemicus* ATCC 39920 cultivation in synthetic medium containing glucose, yeast extract, and salts. The cultivations were carried out at noncontrolled pH (acidifying cultivation) and pH controlled at 7.0 over 24 h, using a 3 L BioFlo III fermentation system (New Brunswick Scientific, Edison, NJ).

HA precipitation

The cultivation broth was centrifuged at 3200 rpm during 20 min. The cell-free broth was treated with ethanol in a proportion 1.5 : 1 v/v ethanol: supernatant. The solution was remained at 4°C during 1 h for precipitation of HA. The precipitated HA was redissolved in a 0.15 mol L⁻¹ NaCl solution. Three steps of precipitation and redissolution were performed to increase the yield of precipitated HA.

Analytical methods

HA concentration

The HA concentration was measured by the carbazole method.¹⁸ Initially the sample was digested with concentrated sulfuric acid and heating. Then the mixture was cooled to room temperature and 0.1% alcoholic solution of pure carbazole (Sigma Chemical Company, MO) was added. After 2 h, the absorbance of the mixture was read on a spectrophotometer at a wavelength of 530 nm. Sodium hyaluronate (HylumedTM, Genzyme, MA) was used as a standard for the calibration curve.

HA molecular weight

The average molecular weight of HA was determined by size exclusion chromatography (SEC). It

was used a Shimadzu chromatography system (Shimadzu, Kyoto, Japan), containing a 7.8 mm × 300 mm Polysep-GFC-P6000 column of the gel filtration (Phenomenex, Torrance, CA) and a refraction index detector (Shimadzu RID-6A). The analysis conditions were: injected sample of 20 μL, 0.1 mol L⁻¹ NaNO₃ as the mobile phase, flow rate of 1.0 mL min⁻¹, and 25°C temperature, as suggested by the column manufacturer. Dextran (American Polymer Standards, Mentor, OH) with molecular weight ranging from 5.2 × 10³ to 7.4 × 10⁶ Da was used as a standard for the calibration curve as described by Balke et al.¹⁹ Molecular weights higher than 7.4 × 10⁶ Da were calculated by extrapolation of the calibration curve.

Protein concentration

The protein content in HA precipitate was determined by UV absorption at 280nm,²⁰ using bovine serum albumin (BSA, Sigma, St. Louis, MO) as a standard.

Rheological analysis: Steady shear tests and dynamic oscillatory tests

Rheological properties were measured by a Haake RheoStress 1 rheometer (Haake, Karlsruhe, BW, Germany). Rheological behavior of the microbial HA in 0.15 mol L⁻¹ NaCl solution was assessed by measuring the oscillatory viscoelastic parameters and the permanent flow analysis at 25°C, using 35-mm parallel plates and gap of 1 mm. Double gap cylinder system (DG43 Ti) was used for lower HA concentration samples, with gap of 5.1 mm and sample volume of 11.5 mL. Oscillatory measurements were conducted in the linear region, at a stress of 1.188 Pa, under a frequency range of 0.1–12.92 Hz. Steady shear measurements were carried out at shear rates of 1–50 s⁻¹.

Atomic force microscopy

In the AFM analysis, the HA precipitate was redissolved in water in all precipitation steps to avoid the presence of NaCl. At the end of the precipitation, the HA precipitate was dissolved at a concentration of 10 mg mL⁻¹ and filtered through 0.45-μm membranes (Sartorius, Goettingen, Germany). The HA solution was diluted to final concentrations of 0.01 and 1 mg mL⁻¹ with 0.01 mol L⁻¹ MgCl₂ solution and equilibrated under magnetic stirring for 16 h at 25°C. After cleavage, mica was hydrated with 100 μL of 0.01 mol L⁻¹ MgCl₂ solution for 15 s which was drained on a filter paper. The surface was rinsed with 3 × 100 μL of deionized water and 70 μL of dilute HA solution was deposited on mica surface, allowed to interact for 5 min, then rinsed with deionized water and dried under a gentle stream of

N₂. The mica surface was used immediately for AFM studies. The AFM instrument was an Autoprobe cp (Park Scientific, Sunnyvale, CA) and images were obtained in air at room temperature and humidity. The tapping mode was employed, using silicon probes of 125- μm nominal length, at a drive frequency of ~ 160 kHz. Data were stored in 256×256 pixel format and images were processed using the Gwyddion software (Gwyddion 2.15, GNU General Public License, <http://www.gwyddion.net>, 2009).

RESULTS AND DISCUSSION

HA pureness characterization for the rheological studies

The protein content in the HA obtained from the *Streptococcus zooepidemicus* ATCC 39920 cultivation was quantified prior to the rheological studies. Aiming to decrease the protein content to reach the medical grade specifications, HA was precipitated with ethanol from the cultivation broths at pH 7.0 and 5.0. Figure 1(a) presents the chromatogram from the UV-vis detector signal at the wavelength 280 nm. The results illustrate the pH influence on the protein concentration in both aspects: the cultivation broths of the *Streptococcus zooepidemicus* ATCC 39920 at acidifying conditions and controlled pH 7.0, as well as on the precipitation with ethanol. The protein contents of HA precipitated at pH 5.0 was 86.4 mg g^{-1} . However, the one from the HA precipitated at pH 7.0 was 0.44 mg g^{-1} which complies with the British Pharmacopeia 2003 specifications²¹ for medical grade HA ($<1 \text{ mg g}^{-1}$). The HA pureness grade may also be observed through the color of the obtained precipitates [Fig. 1(b,c)]. The strong reduction of the color identifies the absence of proteins and the other contaminants.

HA molecular weight

The HA average molecular weight (MW) in the end of cultivations was 4.0×10^6 Da and 2.1×10^7 Da, for controlled pH 7.0 cultivation and precipitation and noncontrolled pH cultivation and precipitation at pH 5.0, respectively.

Rheological characteristics of microbial HA

Once the rheology of HA solutions is extremely sensitive to protein contamination, the polymer produced in the controlled pH cultivation (lower protein content) was used in determination of the main rheological characteristics.

Shear flow measurements

Shear-thinning (viscosity decreasing with increasing of the shear rate) is a well-known polymer solutions

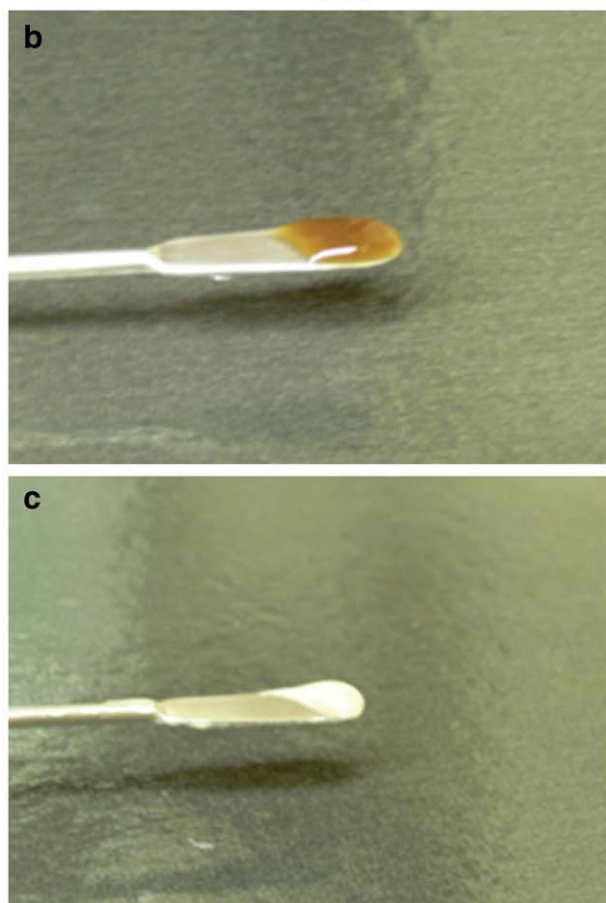
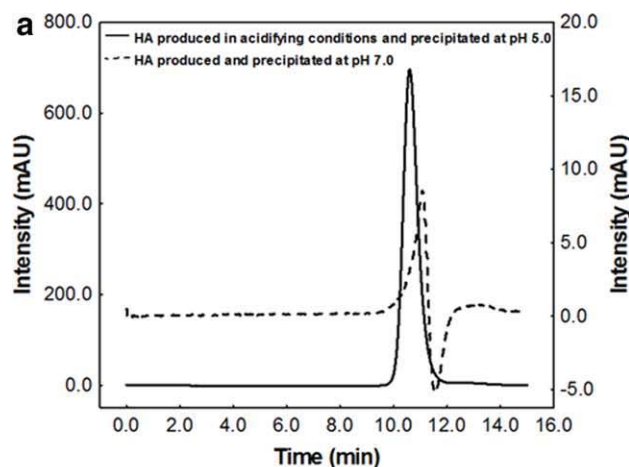


Figure 1 The pH effects on (a) the protein content and (b,c) the color of the obtained precipitates from the *Streptococcus zooepidemicus* ATCC 39920 (—, b) cultivation in acidifying conditions precipitated at pH 5.0; (---, c) cultivation and precipitation at pH 7.0. The intensity measurements were obtained from a UV-vis detector at 280 nm. [Color figure can be viewed in the online issue, which is available at wileyonlinelibrary.com.]

property²² which is typical of entangled networks. In these networks, the rheological response is controlled by the entanglement formation and disruption rates. At low shear the two rates are similar while with the increasing of the shear rate, the

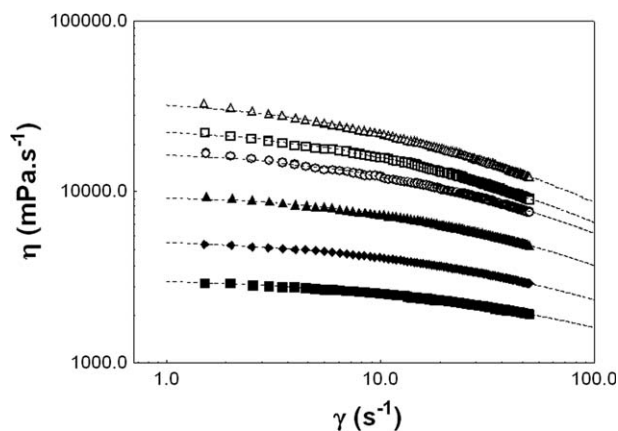


Figure 2 Flow curves for microbial HA at different concentrations in 0.15 mol L⁻¹ NaCl solution at 25°C: (■) 50; (◆) 60; (▲) 70; (○) 80; (□) 90; (△) 100 mg mL⁻¹. All concentrations are expressed as mg mL⁻¹. Dotted lines represent predictions of the Cross model.

disruption rate becomes predominant, leading to thinning.¹⁷ Figure 2 shows this rheological behavior for the higher HA concentrations studied.

The flow curves can be fitted by the Cross equation²³:

$$\eta - \eta_{\infty} / \eta_0 - \eta_{\infty} = 1 / [1 + (\tau\gamma)^m]$$

where η is the viscosity of the system measured at the shear rate γ , η_0 is the initial plateau Newtonian viscosity, η_{∞} the limiting Newtonian viscosity at high shear rates ($\eta_{\infty} \ll \eta_0$; we took $\eta_{\infty} = 0$), τ a characteristic time related to the longest relaxation time of the system, and m a dimensionless exponent which is about 0.60–0.70 for typical polymer solutions.²⁴ The parameters (Table I) were obtained by fitting the Cross model to the data and a value between 0.01 and 0.05 s was found for τ , while m ranged from 0.59 to 0.69 for the higher HA concentrations studied. For example, values of τ and/or m in this range have been quoted for locust bean gum²⁵ and gelatin-locust bean gum system.²⁴ These values also compare with that reported by Oblonšek et al.²⁶ for substituted guar gum. Similar results have been found for synovial fluid,²⁷ whose concentration of HA ranged from 1.4 to 3.6 g L⁻¹.²⁸

The increase in η_0 was observed with increasing concentrations, as expected. With enhancing concentration, individual random coils in a polymer solution start to overlap and interpenetrate one another. It leads to the formation of entanglements, consequently causing the viscosity to increase. Since the freedom of movement of individual chains is progressively restricted, consequent increase in the time required to form new entanglements to replace those disrupted by externally imposed shear is observed and the structural relaxation time (τ) increases with

TABLE I
Regressed Parameter Values of Cross Viscosity Model Fitting to the Flow Curves for Microbial HA Solutions in 0.15 mol L⁻¹ NaCl at 25°C

HA concentration (mg mL ⁻¹)	η_0 (mPa s ⁻¹)	τ (s)	m	R^2
50	3181.7	0.01	0.59	0.9997
60	5454.8	0.02	0.61	0.9999
70	9958.6	0.02	0.68	0.9932
80	18261.4	0.03	0.65	0.9920
90	25161.1	0.05	0.68	0.9989
100	36413.4	0.05	0.69	0.9945

concentration.²⁹ Therefore, the shear rate at which the behavior becomes non Newtonian shifts to a lower value as concentration increases.³⁰ The value of m indicates the degree of shear-thinning behaviors. It approaches zero for Newtonian fluids, whereas shear-thinning materials have a positive m mostly below unity.²⁹

The concentration dependence of η_{sp} defines the fractional increase in viscosity due to the presence of the polymer. Morris et al.³¹ observed that this dependence shows similar behaviors for various random-coil polysaccharides such as dextran and alginate. In this study, the same behavior was also observed (Fig. 3). Two distinct slope linear regimes may be identified which are consistent with data reported by Morris et al.³¹ The first regime with a slope of 1.02 corresponds to the dilute solution where isolated chains are present. The second one with a slope of 3.09 represents semidilute solutions. Morris et al.³¹ found a slope of 1.4 in the dilute solution for all polymers studied, while in the concentrated region the slope increased to 3.3. Dobrynin et al.³² predict for polyelectrolytes in the high-salt limit, $\eta \sim c^{5/4}$ for semidilute unentangled solution and $\eta \sim c^{15/4}$ for semidilute entangled solution,

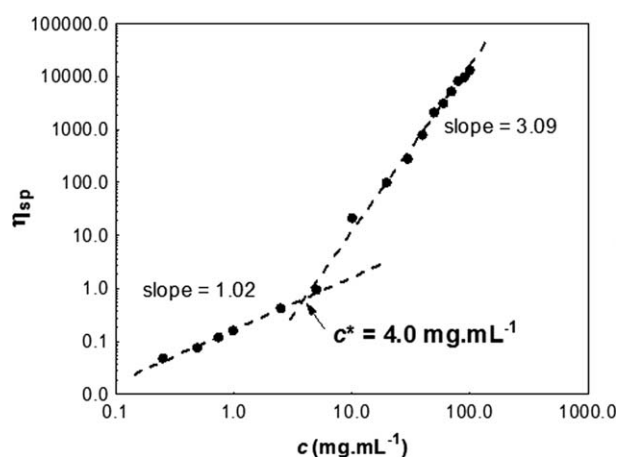


Figure 3 The concentration dependence of the specific viscosity (η_{sp}) for the microbial HA in 0.15 mol L⁻¹ NaCl solution at 25°C.

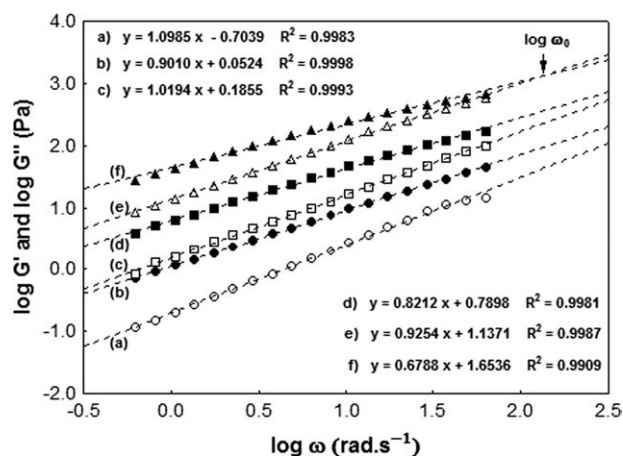


Figure 4 Storage (open symbol) and loss (closed symbol) shear moduli of microbial HA solutions in 0.15 mol L⁻¹ NaCl at 25°C as a function of angular frequency: (○) 40; (□) 60; (△) 100 mg mL⁻¹. All concentrations are expressed as mg mL⁻¹. The model fit and their equations are showed: (a) G'—40 mg mL⁻¹; (b) G''—40 mg mL⁻¹; (c) G'—60 mg mL⁻¹; (d) G''—60 mg mL⁻¹; (e) G'—100 mg mL⁻¹; (f) G''—100 mg mL⁻¹.

identical to the scaling predictions for uncharged polymers in good solvent presented by Colby et al.³³ because the electrostatic interactions are thought to be analogous to excluded volume.

From the two straight-lines intersection (Fig. 3) the critical overlap concentration (c^*) was calculated to be 4.0 mg mL⁻¹. The c^* corresponds to the concentration at which the chains start to overlap and the free motion of a single chain is restricted by the presence of the others. This value is close to that estimated by Mo et al.,³⁴ 2 mg mL⁻¹, for HA in 0.1 mol L⁻¹ NaCl solution at 20°C with MW of 2.0 × 10⁶ Da.

Dynamic measurements

In this work, both (G') and (G'') moduli increased with frequency (Fig. 4). Since the storage modulus usually represents the elastic character and the loss modulus describes the viscous behavior, this result suggests that the enhancement in structural entanglement increases the G' modulus, while structural breakdown increases the G'' modulus.³⁵ In addition, with increasing HA concentration, the moduli at the same angular frequency increased.

Dynamic rheological tests also showed that the magnitudes of G'' were greater than those of the G' for the other concentrations, in all of the angular frequency studied range (Fig. 4). HA solutions with concentration below 10 mg mL⁻¹ showed unsatisfactory results with oscillations in dynamic rheological tests due to the rheometer sensitivity and limitations in the used geometry.

TABLE II
 G' and G'' slopes and intercepts determining the cross-over frequency (ω_0) from microbial HA solutions in 0.15 mol L⁻¹ NaCl at 25°C

HA concentration (mg mL ⁻¹)	G'		G''		Intercept (log ω_0)
	Slope	R^2	Slope	R^2	
40	1.099	0.9983	0.901	0.9998	3.83
50	1.030	0.9980	0.848	0.9985	3.50
60	1.019	0.9993	0.821	0.9981	3.09
70	1.016	0.9997	0.781	0.9949	2.67
80	0.999	0.9995	0.740	0.9935	2.40
90	0.966	0.9989	0.726	0.9912	2.35
100	0.925	0.9987	0.679	0.9909	2.09

Although G' and G'' values were similar, the G' were slightly higher than the G'' slopes for each concentration (Fig. 4), indicating that a probable cross-over point at frequency ω_0 should take place at frequencies higher than the studied range. According to the estimated intercepts in Table II, the crossover frequency (ω_0) should decrease with the increasing HA concentration.

As shown in Figure 5, measured values of log G' for HA in 0.15 mol L⁻¹ NaCl solution at 25°C increased linearly along with the polymer concentration logarithm (log c). Slopes of the double-logarithmic plot close to value 2 are often observed for biopolymers with a large number of potential binding sites along each chain (i.e., high “functionality”) at concentrations substantially higher than the minimum required for a continuous network formation.³⁶ In this work, the slope was 4.18 which suggests a very coiled polymer with intense intra and intermolecular chain interactions. According to Bozzi et al.³⁷ these high values are due to an increase in the yield of crosslinks when polymer concentration increases. Xu et al.³⁸ found a slope of 3.97 for the A gum, exopolysaccharide produced by *Aeromonas nichidenii* 5797, at 25°C.

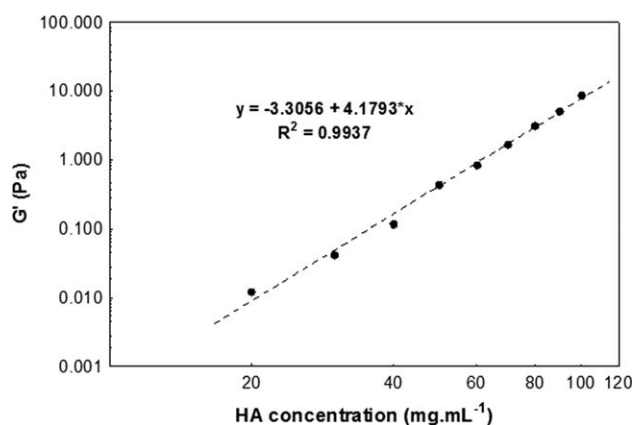


Figure 5 The concentration dependence of the storage modulus (G') for microbial HA in 0.15 mol L⁻¹ NaCl solution at 25°C, measured at frequency of 0.63 rad s⁻¹.

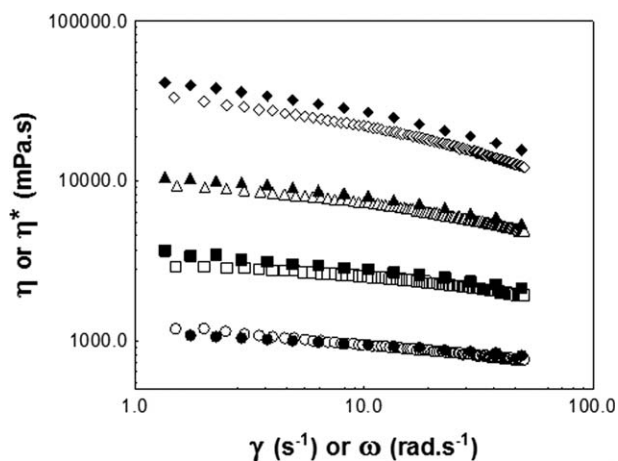


Figure 6 Cox-Merz plot of the microbial HA in 0.15 mol L⁻¹ NaCl solution at 25°C, with various concentrations: (○) 40; (□) 50, (△) 70; (◇) 100 mg mL⁻¹. All concentrations are expressed as mg mL⁻¹. Open symbol: η ; Closed symbol: η^* .

It is of interest to determine the relationship between the rheological parameters determined from oscillatory tests such as complex viscosity (η^*) and the apparent viscosity (η), from steady shear flow tests.³⁹ The superimpositions of η and η^* at equal values of frequency (ω) and shear rate (γ) are known as the Cox-Merz rule, defined by eq. (1).

$$|\eta^*(\omega)| = \eta(\gamma = \omega)$$

This empirical correlation was found to be applicable to fluids with a homogeneous structure, such as random-coil polysaccharide solutions.³¹ Good superposition of η (γ) and η^* (ω) was found only for the lower HA concentrations as 40 mg mL⁻¹ (Fig. 6). Deviations in behavior from theoretical predictions, as observed for the higher HA concentrations, occur for biopolymer dispersions with either hyperentanglements (i.e., high density entanglements) or

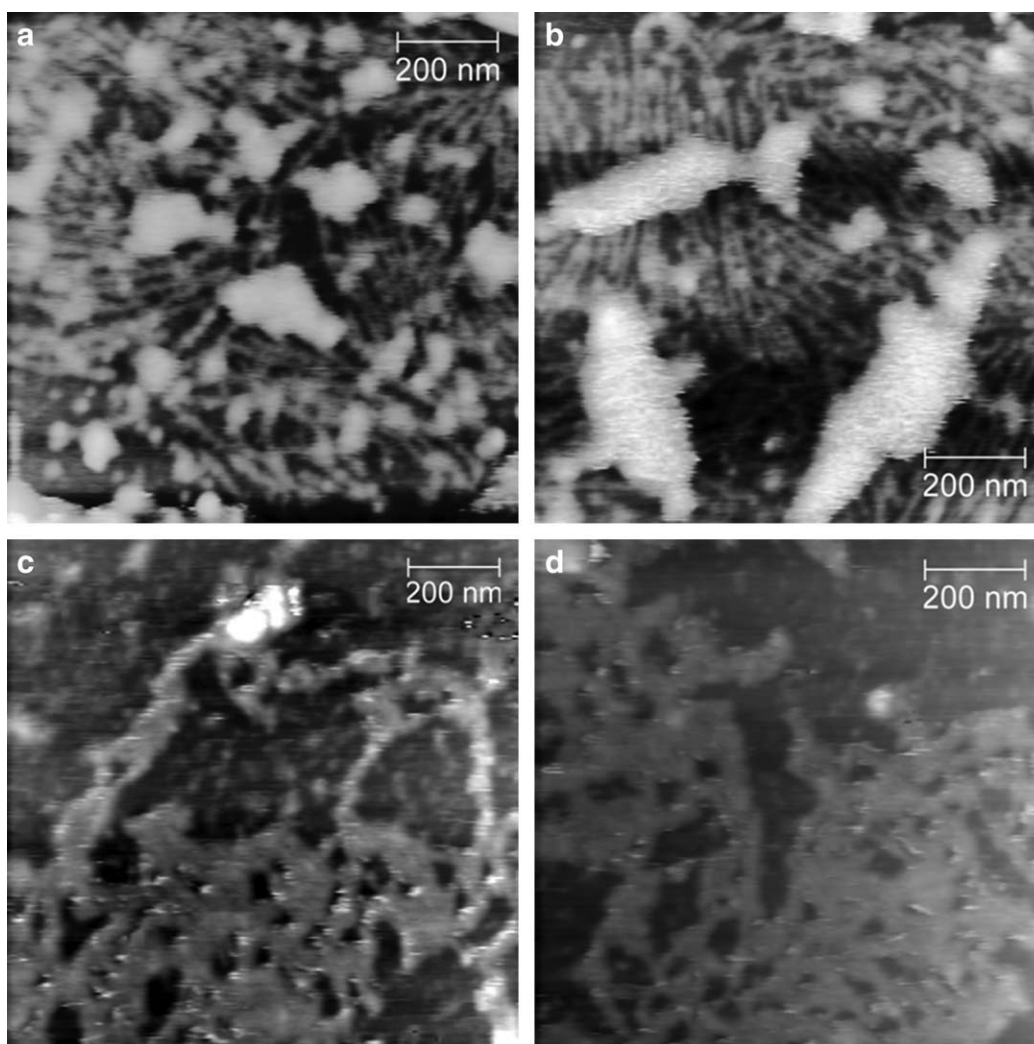


Figure 7 Networks formed by microbial HA in 0.01 mol L⁻¹ MgCl₂ solution deposited on mica: (a-b) 0.01 mg mL⁻¹; (c-d) 1.0 mg mL⁻¹. Height image 1 $\mu\text{m} \times 1 \mu\text{m}$.

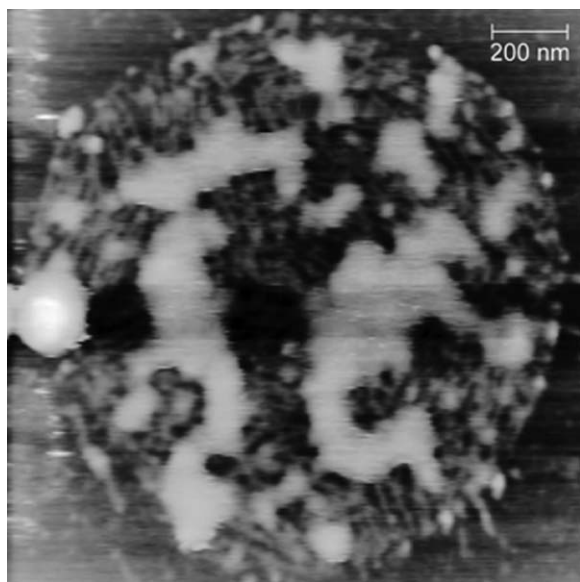


Figure 8 Clusters of microbial HA chains observed when 0.01 mg mL^{-1} HA solution were deposited on mica. Height image $1.5 \mu\text{m} \times 1.5 \mu\text{m}$.

aggregates⁴⁰ whenever η^* is higher than η at equivalent rates of deformation indicating a tenuous network which remains its integrity under low-amplitude oscillation but is disrupted by continuous shear.⁴¹

The microbial HA conformations

HA in diluted solutions was observed through the tapping mode atomic force microscopy (AFM) in air. Although the concentrations of the solutions of HA were below the critical overlap concentration, isolated chains could not be observed due to the tremendous tendency of the HA chains to self-associate, forming networks of fibrils and fenestrated structures as may be seen in Figure 7. This behavior was also observed by Cowman et al.³ and Jacoboni et al.,⁴² when HA was deposited on mica and studied under butanol or in air through a thin layer of water existing on the mica surface.

Although the qualitative nature of the analysis, the thickness of the strands increased with the HA concentration (Fig. 7), as described by Scott et al.² Large spherical shape clusters of HA chains with diameters of $1.4 \mu\text{m}$ were observed even at low HA concentrations as 0.01 mg mL^{-1} (Fig. 8).

CONCLUSIONS

The rheological analysis has been a useful tool to explore relationships between mechanical behavior and structure, concentration and molecular weight of the HA produced by *Streptococcus zooepidemicus* ATCC 39920 in cultivation performed at constant pH 7.0 followed by precipitation with ethanol at pH 7.0.

The concentration dependence of specific viscosity (η_{sp}) showed behavior similar to most random-coil polysaccharide solutions and polyelectrolytes. Frequency sweeps showed a concentration dependence, with the storage (G') and loss (G'') moduli increasing along with the HA concentration. Estimates out the studied range indicate that the crossover frequency should decrease with the increasing HA concentration.

The G' slope along with HA concentration was above the c^2 -dependence often observed for biopolymers with high functionality. Regarding the correlation between the rheological parameters determined from oscillatory and steady shear flow tests, the Cox-Merz rule was not obeyed for the majority of concentrations. Thus, the deviations of the Cox-Merz rule as well as the high concentration dependence of G' confirm the high entanglements density of the HA chains. Large spherical shape clusters of chains were observed through AFM even at 0.01 mg mL^{-1} HA concentrations.

These results contribute to a better understanding of the rheological HA behavior in solution, which is of extreme importance for specific medical and cosmetic applications.

The authors acknowledge the Investiga Group (Campinas, São Paulo, Brazil) for the maintenance of the bacteria culture. They also thank Prof. Dr. Edvaldo Sabadini (Institute of Chemistry, University of Campinas) for the permission of the use of rheometer, Prof. Dr. Mônica Cotta (Institute of Physics, University of Campinas) for the permission of the use of atomic force microscope, and Angela Klatil Ribeiro for the language review.

References

- Garg, H. G.; Hales, C. A. *Chemistry and Biology of Hyaluronan*; Elsevier: Oxford, 2004.
- Scott, J. E.; Cummings, C.; Brass, A.; Chen, Y. *Biochem J* 1991, 274, 699.
- Cowman, M. K.; Spagnoli, C.; Kudashveva, D.; Li, M.; Dyal, A.; Kanai, S.; Balazs, E. A. *Biophys J* 2005, 88, 590.
- Krause, W. E.; Bellomo, E. G.; Colby, R. H. *Biomacromolecule* 2001, 2, 65.
- Gómez-Alejandre, S.; Sánchez, E.; Abradelo, C.; Rey-Stolle, M. F.; Hernández-Fuentes, I. *Int J Biol Macromol* 2000, 27, 287.
- Cowman, M. K.; Li, M.; Dyal, A.; Kanai, S. In *Hyaluronan*; Kennedy, J. J., Phillips, G. O., Williams, P. A., Eds.; Woodhead Publishing: Cambridge, 2002; p 109.
- Hascall, V. C.; Laurent, T. C. In *Science of Hyaluronan Today*; Hascall, V. C., Yanagishita, M., Eds.; Seikagaku Corp.: Tokyo, 1997. Available at: www.glycoforum.gr.jp/science/hyaluronan/hyaluronanE.html.
- Cowman, M. K.; Matsuoka, S. In *Hyaluronan*; Kennedy, J. J., Phillips, G. O., Williams, P. A., Eds.; Woodhead Publishing: Cambridge, 2002; p 75.
- Balazs, E. A.; Gibbs, D. A. In *Chemistry and Molecular Biology of the Intercellular Matrix*; Balazs, E. A., Ed.; Academic Press: London, 1970; p 1241.

10. Armstrong, D. C.; Johns, M. R. *Appl Environ Microbiol* 1997, 63, 2759.
11. Maltese, A.; Borzacchiello, A.; Mayol, L.; Bucolo, C.; Maugeri, F.; Nicolais, L.; Ambrosio, L. *Biomaterials* 2006, 27, 5134.
12. Kelly, M. A.; Kurzweil, P. R.; Moskowitz, R. W. *Am J Orthop* 2004, 33, 15.
13. Kanchwala, S. K.; Holloway, L.; Bucky, L. P. *Ann Plast Surg* 2005, 55, 30.
14. Esposito, E.; Menegatti, E.; Cortesi, R. *Int J Pharm* 2005, 288, 35.
15. Falcone, S. J.; Palmeri, D. M.; Berg, R. A. *J Biomed Mater Res* 2006, 76A, 721.
16. Chamberlain, E. K.; Rao, M. A. *Food Hydrocoll* 2000, 14, 163.
17. Ambrosio, L.; Borzacchiello, A.; Netti, P. A.; Nicolais, L. J.; *Macromol Sci Pure Appl Chem* 1999, A36, 91.
18. Dische, Z. *J Biol Chem* 1946, 167, 189.
19. Balke, S.; Hamielec, A.; Leclkaier, B.; Pearce, S. *Ind Eng Chem Prod Res Dev* 1969, 8, 54.
20. Stoscheck, C. M. *Methods Enzymol* 1990, 182, 50.
21. Rangaswamy, V.; Jain, D. *Biotechnol Lett* 2008, 30, 493.
22. Macosko, C. W. *Rheology. Principles, Measurements, and Applications*; VCH Publishers: New York, 1994.
23. Cross, M. M. *J Colloid Sci* 1965, 20, 417.
24. Alves, M. M.; Garnier, C.; Lefebvre, J.; Gonçalves, M. P. *Food Hydrocolloids* 2001, 15, 117.
25. Sittikijyothin, W.; Torres, D.; Gonçalves, M. P. *Carbohydr Polym* 2005, 59, 339.
26. Oblonšek, M.; Šostar-Turk, S.; Lapasin, R. *Rheol Acta* 2003, 42, 491.
27. Barnes, H. A.; Walters, K. *Rheol Acta* 1985, 24, 323.
28. Kogan, G.; Šoltés, L.; Stern, R.; Gemeiner, P. *Biotechnol Lett* 2007, 29, 17.
29. Lee, S.; Warner, K.; Inglett, G. E. *J Agric Food Chem* 2005, 53, 9805.
30. Gorret, N.; Renard, C. M. G. C.; Famelarta, M. H.; Maubois, J. L.; Doublier, J. L. *Carbohydr Polym* 2003, 51, 149.
31. Morris, E. R.; Cutler, A. N.; Ross-Murphy, S. B.; Rees, D. A.; Price, J. *Carbohydr Polym* 1981, 1, 5.
32. Dobrynin, A. V.; Colby, R. H.; Rubinstein, M. *Macromolecules* 1995, 28, 1859.
33. Colby, R. H.; Rubinstein, M.; Daoud, M. J. *J Phys II* 1994, 4, 1299.
34. Mo, Y.; Takaya, T.; Nishinari, K.; Kubota, K.; Okamoto, A. *Biopolymers* 1999, 50, 23.
35. Rwei, S. P.; Chen, S. W.; Mao, C. F.; Fang, H. W. *Biochem Eng J* 2008, 40, 211.
36. Hember, M. W. N.; Morris, E. R. *Carbohydr Polym* 1995, 27, 23.
37. Bozzi, L.; Milas, M.; Rinaudo, M. *Int J Biol Macromol* 1996, 18, 83.
38. Xu, X.; Liu, W.; Zhang, L. *Food Hydrocoll* 2006, 20, 723.
39. Lopes Da Silva, J. A.; Rao, M. A. In *Food Polysaccharides and their Applications*, 2nd ed.; Stephen, A. M., Williams, P. A., Eds.; Marcel Dekker: New York, 2006.
40. Yoo, B.; Yoo, D.; Kim, Y. R.; Lim, S. T. *Food Sci Biotechnol* 2003, 12, 316.
41. Chronakis, I. S.; Kasapis, S. In *Food Flavors: Generation, Analysis and Process Influence*; Charalambous, G., Ed.; Elsevier: Amsterdam, 1995; p 75.
42. Jacoboni, I.; Valdè, U.; Mori, G.; Quaglino, D.; Jr. Pasquali-Ronchetti, I. J. *J Struct Biol* 1999, 126, 52.